Analysis of chaotic motion and its shape dependence in a generalized piecewise linear map

S. Rajagopalan* and M. Sabir†
Department of Physics, Cochin University of Science and Technology, Cochin 682 022, Kerala, India
(Received 2 October 2000; published 25 April 2001)

We analyze the chaotic motion and its shape dependence in a piecewise linear map using Fujisaka's characteristic function method. The map is a generalization of the one introduced by Artuso. Exact expressions for diffusion coefficients are obtained with previously obtained results used as special cases. A fluctuation spectrum relating to the probability density function is obtained in a parametric form. We also give limiting forms of the above quantities. The dependence of the diffusion coefficient and probability density function on the shape of the map is examined.

DOI: 10.1103/PhysRevE.63.057201 PACS number(s): 05.45.−a, 05.40.−a, 05.60.−k, 45.05.+x

Deterministic diffusion is a well-known phenomenon in spatially extended, one-dimensional maps [1–8]. It has been proposed as a possible mechanism to account for the behavior of Josephson junctions in the presence of microwave radiation [9] and of parametrically driven oscillators [10]. In Hamiltonian dynamics [11], transport due to chaos is also significant because of its applications in celestial mechanics, confinement problems, and so on. Recently, some exactly solvable models have been analyzed [6–8]. The only aim of these studies is the evaluation of the exact diffusion coefficient using a cycle expansion technique [12]. It is a well-known fact that the chaotic dynamics in spatially extended maps has two complementary aspects—diffusion and intermittency. These are related to the probability distribution, which is approximately Gaussian by the central limit theorem. Fujisaka's characteristic function method is a useful tool for analyzing both these aspects of stochasticity in such maps. In this brief report, we apply the characteristic function formalism [13,14] to analyze the chaotic motion in a generalized piecewise linear (GPL) map with a variable shape. It is a generalization of the exactly solvable model in Ref. [6] allowing analytical study. The exact expression for the diffusion coefficient and a parametric representation for the fluctuation spectrum relating to the probability density function (PDF) are obtained. Generalization permits the study of the dependence of these quantities on the shape of the map. We notice that the GPL map with flat peaks is more suited to describe systems exhibiting intermittency in time. The generalization brings the map in Ref. [6] nearer to sinusoidal maps studied numerically in Ref. [1]. A similar shape dependent piecewise linear model has been examined in Ref. [2] from the point of view of correlation times.

Chaos-induced diffusion systems have a general form [4,13]:

$$X_{t+1}=X_t+P_r(X_t)=Y_r(X_t), \quad P_r(X+1)=P_r(X), \quad (1)$$

where r is a control parameter. The sinusoidal map $P_r(X)=r\sin(2\Pi X)$ is an example [1]. After the decomposition $X_t=N_t+x_t$, where N_t is the cell number measured in which X_t is located and $x_t(0\leqslant x_t<1)$ the distance measured from the relative origin $X=N_t$, Eq. (1) can be uniquely rewritten as two dynamical laws:

$$N_{t+1}=N_t+\Delta(x_t), \quad x_{t+1}=f(x_t). \quad (2)$$

Here $\Delta(x)$ is the jumping number defined as the largest integer smaller than $x+P_r(x)$ and is free from N_t and $f(x)=x+P_r(x)-\Delta(x)$, satisfying $0\leqslant f(x)<1$. $f(x)$ is the reduced map of the extended map (1).

We analyze a piecewise linear map with variable shapes of the type in Fig. 1. In the general case, the map consists of linear segments with slopes $\pm m_i$, $i=0,1,\ldots,h$, $m_i<m_{i-1}$. For the cells on the bisector, the slope magnitude is m_0. For the ith cell above and below this cell on bisector, the slope magnitude changes to m_i. The reduced map consists of $k=4h+3$ linear segments. For k increasing from 1 to $4h+3$, these line segments have slopes $m_0,m_1,m_2,\ldots,m_h,-m_h,-m_{h-1},\ldots,0,-m_1, -m_2,\ldots,-m_h,m_h,m_{h-1},\ldots,m_2,m_1,m_0$, and m_is satisfy the relation

$$\frac{3}{m_0}+\sum_{i=1}^{h}\frac{4}{m_i}=1. \quad (3)$$

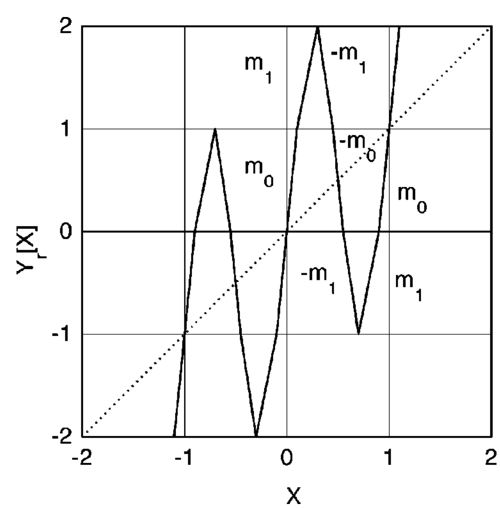

FIG. 1. Generalized piecewise linear (GPL) map with a variable shape with $h=1$. On both axes, units are arbitrary.

*Permanent address: Department of Physics, Sreekrishna College, Guruvayur 680 102, Kerala, India. Email address: srgopal9999@yahoo.com
†Email address: msr@cusat.ac.in FAX: 0484-532495.

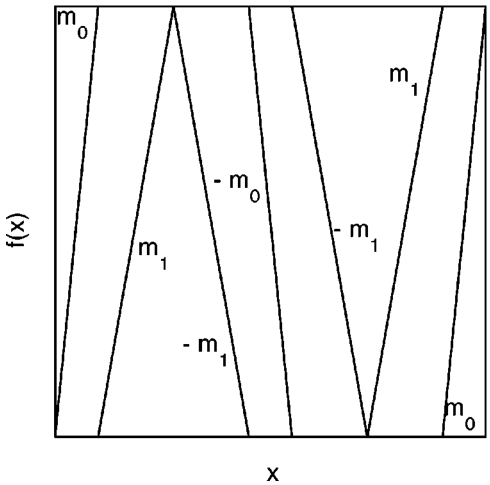

FIG. 2. Reduced map of GPL map in Fig. 1. On both axes, units are arbitrary.

The extended map can be generated from the reduced map by giving suitable jump numbers $\Delta(x)$ (constant for a line segment). These (from left) are $0,1,2,\ldots,h$, $h,h-1,\ldots,2,1,0,-1,-2,\ldots,-h,-h,-(h-1),\ldots,-2$, $-1,0$. Figures 1 and 2 show the map and the reduced map for $h=1$.

The map (1) can be studied using the characteristic function formalism [13,14]. In this, the dynamics of A_t governed by $A_{t+1}=B(x_t)A_t\,(t=0,1,2,\ldots)$ with $A_0=1$ is studied. $B(x_t)$ is a steady function of x_t that evolves according to the chaotic map $x_{t+1}=f(x_t)(0\leqslant x_t<1)$ [13]. Equivalently, one can consider the dynamics of the local time average of a time series $\alpha_t=(1/t)\Sigma_{j=1}^{t}\ln B(x_j)$ [14]. Map (1) can be treated by putting $A_t=\exp(N_t-N_0)$ and $B(x)=\exp[\Delta(x)]$. We put $N_0=0$, and then $\alpha_t=N_t/t$. The long-time dynamics of N_t can be studied using Fujisaka's characteristic function

$$\lambda_q=\frac{1}{q}\lim_{t\to\infty}\frac{1}{t}\ln[\langle\exp(qN_t)\rangle]. \tag{4}$$

$\langle\exp(qN_t)\rangle$ is the average over a steady ensemble and is the q-order moment of $\exp(N_t)$. One can expand λ_q in the series of cumulants. The expansion converges for $|q|<c$, c being the convergence radius. In this case, λ_q can be approximated as

$$\lambda_q=\lambda_0+D\,q, \tag{5}$$

$$\lambda_0=\alpha_\infty=\lim_{t\to\infty}\frac{N_t}{t},$$

where λ_0 is the drift velocity. D is the diffusion coefficient given by

$$\sigma_t=\langle(N_t-\lambda_0 t)^2\rangle\approx 2D\,t \tag{6}$$

for large values of t. σ_t is the variance of N_t. The asymptotic PDF of α_t has a Gaussian component (central limit theorem) and a non-Gaussian component. For $|q|\ll c$, the moment $\langle\exp(qN_t)\rangle$ is determined by the Gaussian component (diffusion branch of q) and for $|q|\gg c$, it is determined by the non-Gaussian component (intermittency branch of q). The PDF $\rho_t(\alpha)$, where α_t takes values between α and $\alpha+d\alpha$, can be obtained as

$$\rho_t(\alpha)\sim\exp[-\sigma(\alpha)t], \tag{7}$$

$\sigma(\alpha)$ being the fluctuation spectrum, $\rho_t(\alpha)\to\delta(\alpha-\alpha_\infty)$ as $t\to\infty$. $\rho_t(\alpha)$ can be obtained from λ_q in parametric form using the Legendre transform

$$\alpha=\frac{d}{dq}(q\lambda_q),$$

$$\sigma(\alpha)=q^2\frac{d}{dq}\lambda_q. \tag{8}$$

We first consider the case with $h=1$. The reduced map consists of seven line segments with slopes (from left) $m_0,m_1,-m_1,-m_0,-m_1,m_1,m_0$. These satisfy Eq. (3). The Frobenius–Perron operator $\mathbf{H}$ is defined by

$$\mathbf{H}G(x)=\sum_{k=1}^{7}\frac{G(y_k)}{|f'(y_k)|}=\sum_{k=1}^{7}\frac{G(y_k)}{|m_k|}, \tag{9}$$

where y_k is the kth solution of $f(y_k)=x$ and $f'(x)=(d/dx)f(x)$. m_k is the slope of the kth line segment of the reduced map. From Eq. (9) we note that the invariant density $p^*(x)$ is uniform $[p^*(x)=1]$ in the interval $0\leqslant x\leqslant 1$ $[\mathbf{H}p^*(x)=p^*(x)]$. The Lyapunov exponent λ can be obtained as

$$\lambda=\frac{3}{m_0}\ln(m_0)+\frac{4}{m_1}\ln(m_1). \tag{10}$$

Since $m_i>1$, we note that $\lambda>0$, and therefore the reduced map is always chaotic. The characteristic function λ_q can be evaluated [13] using the linear operator defined by Mori *et al.* [15]:

$$\hat{\mathbf{H}}F(x)=\frac{1}{p^*(x)}\mathbf{H}[p^*(x)F(x)], \tag{11}$$

$$\lambda_q=\frac{1}{q}\lim_{t\to\infty}\frac{1}{t}\ln\langle e^{q\Delta x}\underbrace{\hat{\mathbf{H}}\,e^{q\Delta x}\hat{\mathbf{H}}e^{q\Delta x}\cdots\hat{\mathbf{H}}e^{q\Delta x}}_{t-1}\rangle. \tag{12}$$

For our model $\mathbf{H}=\hat{\mathbf{H}}$. $\Delta(x)$, which are constant over a line segment, are (from left) $0,+1,+1,0,-1,-1,0$. Hence we get from Eqs. (9), (11), and (12),

$$\hat{\mathbf{H}}e^{q\Delta x}=\frac{3}{m_0}+\frac{2}{m_1}e^{q}+\frac{2}{m_1}e^{-q}=\frac{3}{m_0}+\frac{4}{m_1}\cosh(q), \tag{13}$$

$$\lambda_q=\frac{1}{q}\ln\left[\frac{3}{m_0}+\frac{4}{m_1}\cosh(q)\right]. \tag{14}$$

The result can be generalized for integer values of h. Again, slopes satisfy relation (3). The Frobenius-Perron operator again leads to the uniform invariant density $p^*(x)=1$. The Lyapunov exponent λ and the characteristic function λ_q are given by

$$\lambda=\frac{3}{m_0}\ln(m_0)+\sum_{i=1}^{h}\frac{4}{m_i}\ln(m_i), \tag{15}$$

$$\lambda_q=\frac{1}{q}\ln\left[\frac{3}{m_0}+\sum_{i=1}^{h}\frac{4}{m_i}\cosh(iq)\right]. \tag{16}$$

The map is fully chaotic since $\lambda>0$. The drift velocity $\lambda_0=0$, always. The diffusion coefficient D is

$$D=\lim_{q\to 0}\frac{d}{dq}\lambda_q=\sum_{i=1}^{h}\frac{2i^2}{m_i}. \tag{17}$$

The fluctuation spectrum $\sigma(\alpha)$ can be gotten in the parametric form using Eq. (8):

$$\alpha=\frac{\sum_{i=1}^{h}(4i/m_i)\sinh(iq)}{3/m_0+\sum_{i=1}^{h}(4/m_i)\cosh(iq)}$$

$$\sigma(\alpha)=q\frac{\sum_{i=1}^{h}(4i/m_i)\sinh(iq)}{3/m_0+\sum_{i=1}^{h}(4/m_i)\cosh(iq)}-\ln\left[\frac{3}{m_0}+\sum_{i=1}^{h}\frac{4}{m_i}\cosh(iq)\right]. \tag{18}$$

$q=0$ gives $\alpha=0$; $\sigma(\alpha)=0$. If $+q$ gives $+\alpha$, $-q$ will give $-\alpha$ without changing $\sigma(\alpha)$. It can also be noted that maximum value of α is obtained by putting $q\to\infty$. We have

$$\alpha_{\max}=h \quad \sigma(\alpha_{\max})=\ln\left(\frac{m_h}{2}\right). \tag{19}$$

In the special case when all m_i's are equal $(=m_0)$, Eq. (17) can be summed to obtain a closed-form expression for D. In this case, Eq. (3) gives $m_0=3+4h$:

$$D=\frac{h(h+1)(2h+1)}{3(4h+3)}. \tag{20}$$

With $h+1=\beta$,

$$D=\frac{(\beta-1)\beta(2\beta-1)}{3(4\beta-1)}, \tag{21}$$

which reduces to $D=2/7$ for $\beta=2$ giving results obtained previously in Ref. [6].

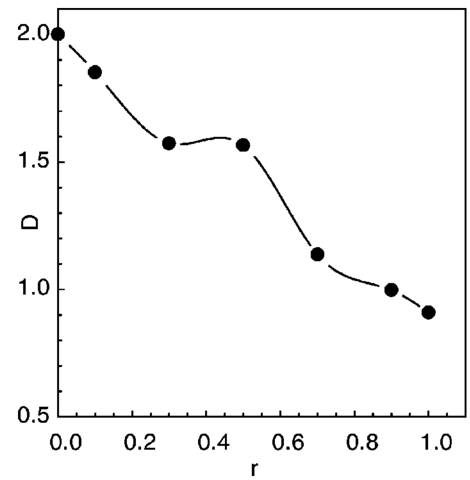

FIG. 3. Variation of diffusion coefficient D with r for $h=2$. On both axes, units are arbitrary.

A closed-form expression can also be gotten for the special case $m_i/m_{i-1}=r=$ a constant, $0<r<1$. Then $m_i=m_0r^i$. From Eq. (3),

$$m_0=3+\frac{4(1-r^h)}{r^h(1-r)}. \tag{22}$$

For every r between 0 and 1, the model becomes an exactly solvable case. From Eq. (17),

$$D=\frac{2[h^2+(1-2h-2h^2)r+(h+1)^2r^2-r^{h+1}-r^{h+2}]}{[3r^h(1-r)+4(1-r^h)](1-r)^2}. \tag{23}$$

The limiting forms of the above quantities can be obtained for a constant h as the peak shape becomes maximum flat. These can be arrived at by taking limit $r\to 0$. From Eq. (23), D behaves like

$$D=\frac{h^2}{2}. \tag{24}$$

The above limit can also be obtained by putting $m_i\to\infty (i=0,\ldots,h-1)$ and $m_h\to 4$. Applying this we get the following limits:

$$\lim_{r\to 0}\lambda_q=\frac{1}{q}\ln[\cosh(qh)], \tag{25}$$

$$\lim_{r\to 0}\alpha=h\tanh(qh), \tag{26}$$

$$\lim_{r\to 0}\sigma(\alpha)=\ln\left[\frac{h^2-\alpha^2}{h^2}\right]^{1/2}\left[\frac{h+\alpha}{h-\alpha}\right]^{\alpha/2h}. \tag{27}$$

In Fig. 3 we plot diffusion coefficient vs r for $h=2$. It can be observed that D increases with increasing flatness of the peak shape. D varies from 0.9 to 2 when r is varied from 1 to 0. Increasing h, keeping $m_i=m_0 (i=1,2,\ldots,h)$ appears to

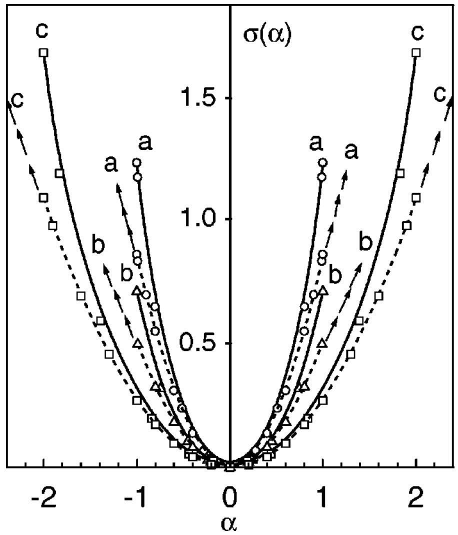

FIG. 4. Fluctuation spectrum $\sigma(\alpha)$ vs α for different cases. Solid lines represent actual $\sigma(\alpha)$ while dotted lines give corresponding Gaussian forms. (a) $h=1$, $m_0=m_1=7$; (b) $h=1$, $m_0=100$, $m_1=4.1237$; and (c) $h=2$, $m_0=m_1=m_2=11$. On both axes, units are arbitrary.

have more influence on increasing D. This is because $D=2/7=0.29$ for $h=1$, whereas it goes to 0.909 for $h=3$ [Eq. (20)].

The probability distribution function for N_t, the distance from the origin, can be obtained using the fluctuation spectrum $\sigma(\alpha)$. From Eq. (7), we have

$$\rho_t(N) \sim \frac{1}{t}\exp\left[-\sigma\left(\frac{N}{t}\right)t\right], \tag{28}$$

$\rho_t(N)$ being the PDF that N_t takes values between N and $N+dN$. This PDF is approximately Gaussian by the central limit theorem. In the exactly normal case λ_q is given by Eq. (5) and $\sigma(\alpha)$ takes the form

$$\sigma(\alpha) = \frac{(\alpha-\lambda_0)^2}{4D} \tag{29}$$

with

$$\alpha = \lambda_0 + 2Dq. \tag{30}$$

For the present model $\lambda_0=0$. In Fig. 4 we plot $\sigma(\alpha)$ for different maps and compare with the Gaussian form given in Eq. (29). For a constant h, the non-Gaussian character increases with increasing flatness of the map. But, as in the case of diffusion coefficients, increasing h has more influence in producing non-Gaussian characters of the PDF.

To conclude, analysis of the PDF with fluctuation spectrum brings out that intermittency and the non-Gaussian character of the PDF increases with increasing peak height and flatness of the map, with height exercising more effect. This is important when one selects models for describing experiments relating to diffusion. For example, systems exhibiting chaotic motion similar to Brownian motion should have a Gaussian distribution. Maps with linear segments having constant slope and minimum peak height are useful in cases like this. Maps with greater height and peaks becoming more flat will be best suited in describing diffusion systems showing intermittency in time. With flatness becoming maximum, the diffusion coefficient behaves like $h^2/2$, h being the peak height. The corresponding limiting forms for the characteristic function and fluctuation spectrum are also obtained. The limiting form of the fluctuation spectrum is quite different from the Gaussian form following the central limit theorem.

We are attempting a generalization of maps with fractional heights given in Ref. [7] along similar lines. This work will be reported elsewhere.

The authors are grateful to University Grants Commission, India, for providing financial assistance through DSA and COSIST schemes.

[1] T. Geisel and J. Nierwetberg, Phys. Rev. Lett. **48**, 7 (1982); M. Schell, S. Fraser, and R. Kapral, Phys. Rev. A **26**, 504 (1982); H. Fujisaka and S. Grossmann, Z. Phys. B: Condens. Matter **48**, 261 (1982).

[2] S. Grossmann and S. Thomae, Phys. Lett. **97A**, 263 (1983).

[3] M. Inoue and H. Koga, Prog. Theor. Phys. **68**, 2184 (1982).

[4] H.G. Schuster, *Deterministic Chaos* (Physik-Verlag, Weinheim, 1984), Chap. 2.

[5] T. Geisel, in *Nonequilibrium Cooperative Phenomena in Physics and Related Fields*, edited by M.G. Velarde (Plenum, New York, 1984).

[6] R. Artuso, Phys. Lett. A **160**, 528 (1991).

[7] H.C. Tseng *et al.*, Phys. Lett. A **195**, 74 (1994).

[8] Chia-Chu Chen, Phys. Rev. E **51**, 2815 (1995).

[9] B.A. Huberman, J.P. Crutchfield, and N.H. Packard, Appl. Phys. Lett. **37**, 750 (1980); M. Cirillo and N.F. Pedersen, Phys. Lett. **90A**, 150 (1982); E. Ben-Jacob *et al.*, Phys. Rev. Lett. **49**, 1599 (1982).

[10] R.W. Leven and B.P. Koch, Phys. Lett. **86A**, 71 (1981).

[11] B.V. Chirikov, Phys. Rep. **52**, 263 (1979).

[12] R. Artuso, E. Aurell, and P. Cvitanovic, Nonlinearity **3**, 325 (1990).

[13] H. Fujisaka, Prog. Theor. Phys. **71**, 513 (1984).

[14] H. Fujisaka and M. Inoue, Prog. Theor. Phys. **77**, 1334 (1987); H. Fujisaka and M. Inoue, *ibid.* **79**, 758 (1988); H. Fujisaka, R. Hagihara, and M. Inoue, Phys. Rev. A **38**, 3680 (1988); H. Fujisaka, A. Yamaguchi, and M. Inoue, Prog. Theor. Phys. **81**, 1146 (1989); H. Shibata, S. Ando, and H. Fujisaka, Phys. Rev. A **45**, 7049 (1992).

[15] H. Mori, B.C. So, and T. Ose, Prog. Theor. Phys. **66**, 1266 (1981).